Since January 2020 Elsevier has created a COVID-19 resource centre with free information in English and Mandarin on the novel coronavirus COVID-19. The COVID-19 resource centre is hosted on Elsevier Connect, the company's public news and information website.

Biomedicine & Pharmacotherapy 155 (2022) 113766

Contents lists available at ScienceDirect

Biomedicine & Pharmacotherapy

journal homepage: www.elsevier.com/locate/biopha

Ganoderma microsporum immunomodulatory protein acts as a multifunctional broad-spectrum antiviral against SARS-CoV-2 by interfering virus binding to the host cells and spike-mediated cell fusion

Ha Phan Thanh Ho [a,1], Di Ngoc Kha Vo [a,1], Tung-Yi Lin [b,c], Jo-Ning Hung [a], Ya-Hui Chiu [a], Ming-Han Tsai [a,c,*]

[a] Institute of Microbiology and Immunology, National Yang Ming Chiao Tung University, Taipei, Taiwan
[b] Institute of Traditional Medicine, National Yang Ming Chiao Tung University, Taipei, Taiwan
[c] Research Center for Epidemic Prevention, National Yang Ming Chiao Tung University, Taipei, Taiwan

ARTICLE INFO

Keywords:
SARS-CoV-2
Fungal immunomodulatory proteins
GMI
Viral binding
Cell fusion
Broad-spectrum antiviral against SARS-CoV-2

ABSTRACT

Background: Severe acute respiratory syndrome coronavirus 2 (SARS-CoV-2) is a highly transmissible coronavirus that has caused over 6 million fatalities. SARS-CoV-2 variants with spike mutations are frequently endowed with a strong capability to escape vaccine-elicited protection. Due to this characteristic, a broad-spectrum inhibitor against SARS-CoV-2 infection is urgently demanded. *Ganoderma microsporum* immunomodulatory protein (GMI) was previously reported to alleviate infection of SARS-CoV-2 through ACE2 downregulation whereas the impact of GMI on virus itself was less understood. Our study aims to determine the effects of GMI on SARS-CoV-2 pseudovirus and the more detailed mechanisms of GMI inhibition against SARS-CoV-2 pseudovirus infection.
Methods: ACE2-overexpressing HEK293T cells (HEK293T/ACE2) and SARS-CoV-2 pseudoviruses carrying spike variants were used to study the effects of GMI *in vitro*. Infectivity was evaluated by fluorescence microscopy and flow cytometry. Fusion rate mediated by SARS-CoV-2 spike protein was examined with split fluorescent protein /luciferase systems. The interactions of GMI with SARS-CoV-2 pseudovirus and ACE2 were investigated by immunoprecipitation and immunoblotting.
Results: GMI broadly blocked SARS-CoV-2 infection in various cell lines. GMI effectively inhibited the infection of pseudotyped viruses carrying different emerged spike variants, including Delta and Omicron strains, on HEK293T/hACE2 cells. In cell-free virus infection, GMI dominantly impeded the binding of spike-bearing pseudotyped viruses to ACE2-expressing cells. In cell-to-cell fusion model, GMI could efficiently inhibit spike-mediated syncytium without the requirement of ACE2 downregulation.
Conclusions: GMI, an FDA-approved dietary ingredient, acts as a multifunctional broad-spectrum antiviral against SARS-CoV-2 and could become a promising candidate for preventing or treating SARS-CoV-2 associated diseases.

1. Introduction

Coronavirus disease-19 (COVID-19), an infectious disease caused by a recently identified virus, namely severe acute respiratory syndrome coronavirus 2 (SARS-CoV-2), has rapidly become a global pandemic, resulting in over 558 million infections and 6 million deaths [1]. SARS-CoV-2 enters and infects host cells mainly through utilizing the interplay between viral spike protein and angiotensin-converting enzyme 2 (ACE2) protein expressed in the target cells [2–4]. The generation of neutralizing antibodies against spike protein offers protection effects by inhibiting spike protein-ACE2 interaction, which ultimately leads to the blockage of SARS-CoV-2 infection [5]. Nevertheless, due to the high mutation rate of RNA genome and the high transmission level of the virus, many SARS-CoV-2 variants had been reported to be highly

Abbreviations: SARS-CoV-2, Severe acute respiratory syndrome coronavirus 2; GMI, *Ganoderma microsporum* immunomodulatory protein; ACE2, Angiotensin-converting enzyme 2; CCZ, Chlorcyclizine; pAb, polyclonal antibody; MG132, Carbobenzoxy-l-leucyl-l-leucyl-l-leucinal; BafA1, Bafilomycin A1.

* Correspondence to: Institute of Microbiology and Immunology, National Yang Ming Chiao Tung University, 155 Li-Nong St., Section 2, Shipai, Beitou, Taipei 112, Taiwan.
E-mail address: m.tsai@nycu.edu.tw (M.-H. Tsai).

[1] These authors equally contribute to this study and are listed alphabetically by last name.

https://doi.org/10.1016/j.biopha.2022.113766
Received 29 August 2022; Received in revised form 19 September 2022; Accepted 26 September 2022
Available online 28 September 2022

resistant to the protection of vaccination [5–9]. Indeed, many of these SARS-CoV-2 strains with immune escape property had accumulated tremendous mutations at their spike proteins and could elude antibodies generated by vaccinating with spike protein derived from the original wildtype strain [8–10]. However, the development of novel vaccines is time-consuming and new viral mutations that lead to vaccine escape could always happen. Consequently, it is crucial to develop other strategies against SARS-CoV-2 infection, such as antiviral drugs. Through high-throughput screening, drug repurposing, and *in silico* prediction, many studies have been conducted to identify potential candidates for inhibiting SARS-CoV-2 infection [11–16]. Despite of the potential effects on viral replication and translation, many of these candidates still lack *in vitro* and *in vivo* experiments to validate their functions, and the requirement of the long period of clinical trials for human usage [13,17,18]. Currently, the approved antiviral drugs focus on blocking viral replication by targeting viral protease or RNA-dependent-RNA polymerase (RdRp), such as Paxlovid and Molnupiravir [19–25]. However, because of the highly mutated nature of RNA viruses, it is predicted that drug-resistant variants could appear after the intensive usage of the antiviral drugs that could only block a single step in the viral life cycle. Likewise, new types of antiviral drugs, especially the ones that are against viral life cycle besides genome replication, are always urgently required. For instance, the antiviral drugs against RNA viruses, such as Human immunodeficiency virus (HIV) and Hepatitis C virus (HCV), were successfully made by combining different drugs against the viral life cycle at different steps [26,27]. Several new antiviral strategies highly focused on inhibiting viral entry through interfering with spike-ACE2 interaction [28–33]. Nevertheless, many of these new strategies still require the strict examinations for efficacy and safety levels before applying for human usage.

We had previously reported that GMI, a fungal immunomodulatory protein from *Ganoderma microsporum*, could alleviate infection of SARS-CoV-2 by inducing ACE2 degradation *in vitro* and in animal models [34]. The downregulation of ACE2 protein could reduce the binding between spike-bearing viruses and the host cells. This finding suggests GMI as a potential candidate for preventing SARS-CoV-2 infection since it is an FDA-approved dietary ingredient with less safety concerns in comparison with the other new drugs regarding prevention purposes [35]. However, it should also be noticed that GMI could only reduce ACE2 protein level by half in the treated samples, and such reduction itself seems impossible to entirely leads to the remarkable inhibition capability against SARS-CoV-2 infection [34]. The results in some ways imply that GMI should have further antiviral strategies against SARS-CoV-2 infections beyond merely downregulating ACE2 protein level.

In this study, HEK293T cells overexpressing ACE2 and SARS-CoV-2 pseudoviruses carrying different spike protein mutations were used to investigate the effects of GMI on SARS-CoV-2 pseudovirus *in vitro* and the more detailed mechanisms of its inhibitory effects against viral infection. We also focused on studying the effects of GMI on viral infection via either cell-free virus or cell-cell fusion, as well as the interactions between GMI and the pseudoviruses. Our results demonstrated that GMI appeared with a broad-spectrum antiviral property against SARS-CoV-2 pseudoviruses expressing different spike variants, including Delta and Omicron strains. The significant effects of GMI were contributed by both viral binding blockage and the inhibition against cell-cell fusion. Without the requirement of downregulating ACE2 expression, GMI could directly impede viral binding and cell fusion by its interaction with both the spike proteins of SARS-CoV-2 pseudoviruses and ACE2 receptor in the target cells. Taken together, GMI could act as a potential inhibitor for SARS-CoV-2 infection and possible pathological consequences related to syncytia formation.

2. Materials & methods

2.1. Cell lines

HEK293 cells are derived from human embryonic kidney cells (ATCCL CRL-1573), and HEK293T is a derivative cell line of HEK293 cells containing the SV40 T-antigen (ATCC: CRL-3216). A549 cells are human lung adenocarcinoma cells derived from a Caucasian lung cancer patient (ATCC: CCL-185). Cells stably expressed with human ACE2 (hACE2), or Spike were acquired after being transduced with lentiviruses carrying hACE2 or spike gene and selected with 10 μg/ml blasticidin (Invitrogen) or 1.5 μg/ml puromycin (Invitrogen), respectively. All cells were cultured in RPMI-1640 medium (Invitrogen) with 10% fetal bovine serum (FBS, HyClone) supplemented with 100 U/ml penicillin and streptomycin (Invitrogen) in a humidified cell culture incubator at 37 °C.

2.2. Reagents and antibodies

GMI (Cat: 767593) was purchased from MycoMagic Biotechnology Co. (Taiwan) and prepared in phosphate-buffered saline PBS (1 mg/ml). The details procedures for GMI generation and its protein structure have been described previously [34]. Chlorcyclizine (CCZ; Cayman#19239), dimethyl sulfoxide (DMSO; Sigma#D8418), carbobenzoxy-L-leucyl-L-leucyl-L-leucinal (MG132; Cayman#13697), and bafilomycin A1 (Baf A1; Cayman#11038). Here a rabbit serum containing polyclonal antibody against the SARS-CoV-2 spike protein (Academia Sinica, Taiwan) was applied for all experiments. GMI-related immunoprecipitation and immumoblotting were performed using a mouse monoclonal antibody against the His-tagged-GMI (clone HIS.H8, Thermo Scientific#MA1–21315). ACE2 polyclonal antibody (Proteintech#21115–1-AP), Anti-rhodopsin 1D4 (Santa Cruz#sc-57432), and mouse gamma globulin as control (ThermoFisher #31878) were used for ACE2 immunoblotting and immunoprecipitation.

2.3. Plasmids and oligonucleotides

pLAS2, a lentiviral vector carrying a CMV promoter was received from Academia Sinica, Taiwan. A green fluorescent protein (GFP) gene or a firefly luciferase gene was therefore inserted after the CMV promoter to create pLAS2-GFP or pLAS2-Luc plasmid. An expression plasmid pcDNA3.1-SARS-CoV-2-Spike contains the wildtype (Wuhan strain) SARS-CoV-2 spike protein with a C-terminal C9 tag (gift from Fang Li; Addgene#145032). D614G or D614G plus N501Y (D614G/N501Y) mutation at Spike gene were performed by polymerase chain reaction (PCR) cloning [36]. The expression plasmid carrying spike gene derived from Beta strain (Academia Sinica, Taiwan), Delta strain (Addgene#179905) or Omicron strain (Addgene#179907) were used [37]. In split GFP system, GFP1–10 plasmid was from Addgene (#68715) while GFP11 plasmid was constructed by gene synthesis. In split Firefly luciferase system, expressing plasmids carrying NFLuc416 and CFLuc398 were constructed in pcDNA3.1 vector. The lenti-ACE2 plasmid (Academia Sinica, Taiwan), and the lenti-Spike plasmid was constructed into pLAS2 plasmid. Final products of PCR cloning would be confirmed by Sanger sequencing. Sequences of all synthesized oligonucleotides are shown in Supplementary Table 1.

2.4. Transfections

All transfection experiments were carried out with polyethylenimine (PEI MAX; Polysciences#24765–1) following the manufacturer's instructions.

2.5. Cell viability assay

5×10^3 cells of the examined cells were seeded into 96-well culture

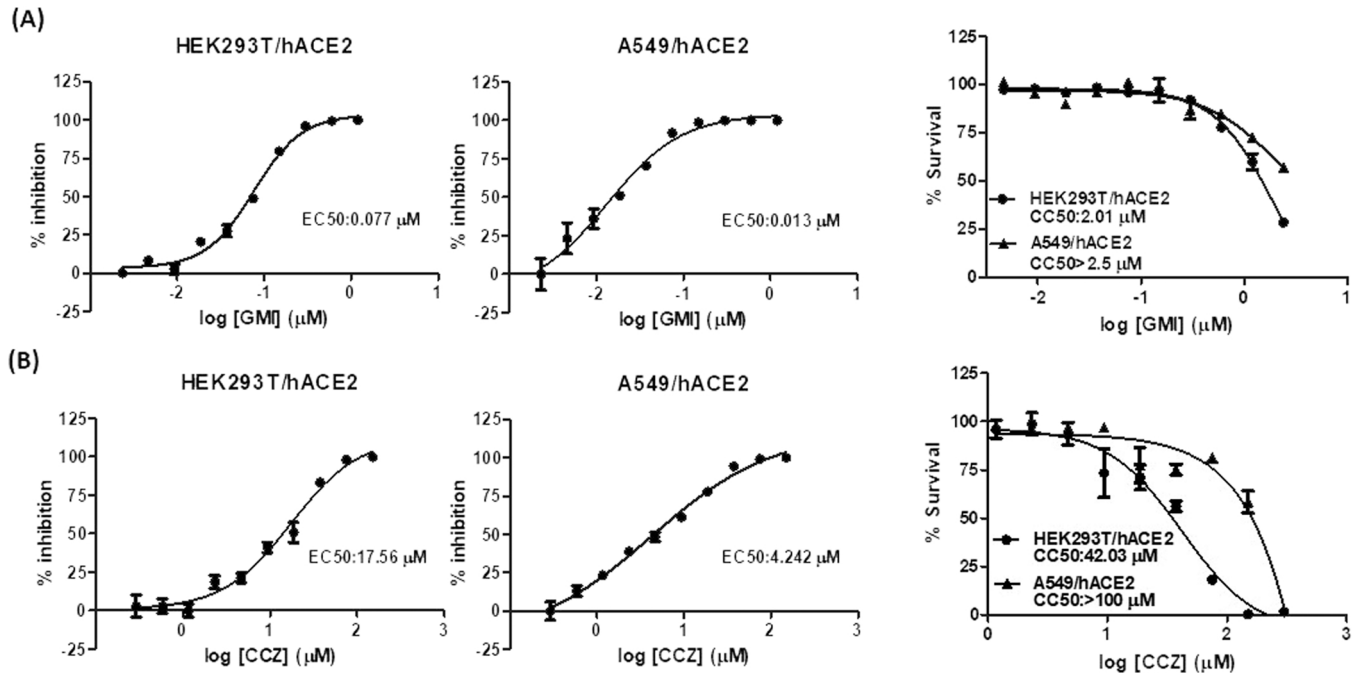

Fig. 1. The inhibition efficacy of GMI and CCZ against SARS-CoV-2 spike-mediated infection in ACE2-expressing human cell lines. HEK293T/hACE2 and A549/hACE2 cells were infected with SARS-CoV-2 pseudotyped virus carrying a luciferase gene with treatment of **(A)** GMI or **(B)** CCZ for 48 h. Luminescent signals of the infected cells were measured 48 h post-infection and EC50 values were calculated using GraphPad Prism 5 software. The cytotoxicity of the cells treated with (A) GMI or (B) CCZ were evaluated 48 h post-treatment through MTT assay and CC50 values were calculated. The data are shown as the means ± SDs (error bars).

plate per well and incubated overnight to allow the cells to reattach. GMI (0–2.4 μM) or CCZ (0–300 μM) were added into the cells as indicated time points, and their survival rates were measured by using MTT assay according to the manufacturer's instructions.

2.6. Pseudovirions and cell infection

Spike pseudovirions were produced as previously reported [36]. Different volumes of pseudovirions were inoculated with 3000 HEK293T/hACE2 cells per well in 96-well plates. 2 days later, transduction efficiency (percentage of GFP-positive cells) was analyzed by a fluorescence microscope (Zeiss) and by flow cytometry (FACSCalibur). For the evaluation of the transduction of luciferase-carry pseudoviruses, the transduced cells were transferred into a 96-well white plate. The relative light unit (RLU) was determined immediately after adding 15 μg/ml VivoGlo™ luciferin (Promega) into the cells by using a multimode microplate reader (SPARK, Tecan Austria GmbH).

2.7. Binding assay

The pseudovirus samples, with or without different inhibitors, were exposed to 20,000 HEK293T/hACE2 cells at 4 °C under constant rotation. 60 min later, the cells were collected by centrifugation, washed with ice-cold PBS for three times, and the viruses-bound cells were collected for immunofluorescence staining and visualized by a fluorescence microscope (Zeiss). In some experiments, these viruses-bound cells were collected for RNA extraction by using GENEzol™ TriRNA Pure kit (Geneaid) and the extracted RNA was further reverse transcribed in cDNA by using random hexamers and RevertAid First Strand cDNA synthesis kit (Thermo Scientific). Reverse transcription-quantitative polymerase chain reaction (RT-qPCR) was performed with ABI StepOnePlus™ System according to SYBR Green method. The amount of RNA corresponding to beta-actin and lentiviral genome was quantified and the binding ability in each sample was calculated through the ratio between viral genome versus beta-actin. The primer sequences applied for RT-qPCR are listed in Supplementary Table 1.

2.8. Fusion assay

In cell-cell fusion assay, HEK293T/spike (effector cells) in 6-well plate were transfected with 1.5 μg each GFP1–10 and CFLuc398 plasmids whereas HEK293T/hACE2 (target cells) were transfected with 1.5 μg each GFP11 and NFLuc416 plasmids. 0.2 μg of mCherry expression plasmid was also co-transfected as a control for transfection efficiency. 24 h later, transfected cells were trypsinized and a total of 5×10^4 cells/well mixed at a 1:1 ratio was cultured in 96-well plate. Cell-cell fusion was evaluated at indicated time points post co-culture by fluorescence microscopy (GFP signals) and by Tecan luminometer (Luciferase activity). Regarding fusion assay of mutated spikes and different spike variants, similar procedures were performed but with HEK293 transfected with expression plasmid carrying spike protein as effector cells. 2 ng of different spike containing plasmids; 1 μg each GFP1–10 and CFLuc398 expressing plasmids, and 0.2 μg of mCherry were used for co-transfection.

2.9. Immunoprecipitation assay

HEK293T cells were transfected with the plasmids encoding different SARS-CoV-2 spikes as indicated. Media were aspirated and replaced with fresh one 24 h later. At 72 h post-transfection, cells were treated with 1.2 μM GMI at 37 °C for 2 h before a complete GMI removal with three PBS washes. Cells were then lysed for 1 h under rotation at 4 °C in 200 μl of lysis buffer (2 mM EDTA, 137 mM NaCl, 20 mM Tris HCl pH 8.0, 1% Nonidet P-40). The lysates were purified with 21,000xg centrifugation in 10 min before immunoprecipitation with Dynabeads Protein G Immunoprecipitation kit (Invitrogen#10007D) according to the manufacturer's instructions. The immunoprecipitated samples were incubated at 95 °C for 20 min in Laemmli buffer before Western blotting.

2.10. Immunoblotting

Cells were lysed on ice for 15 min with a self-prepared lysis buffer (20 mM Tris-HCl pH 7.5, 0.1% SDS, 5 mM EDTA, 0.5% Nonidet P-40,

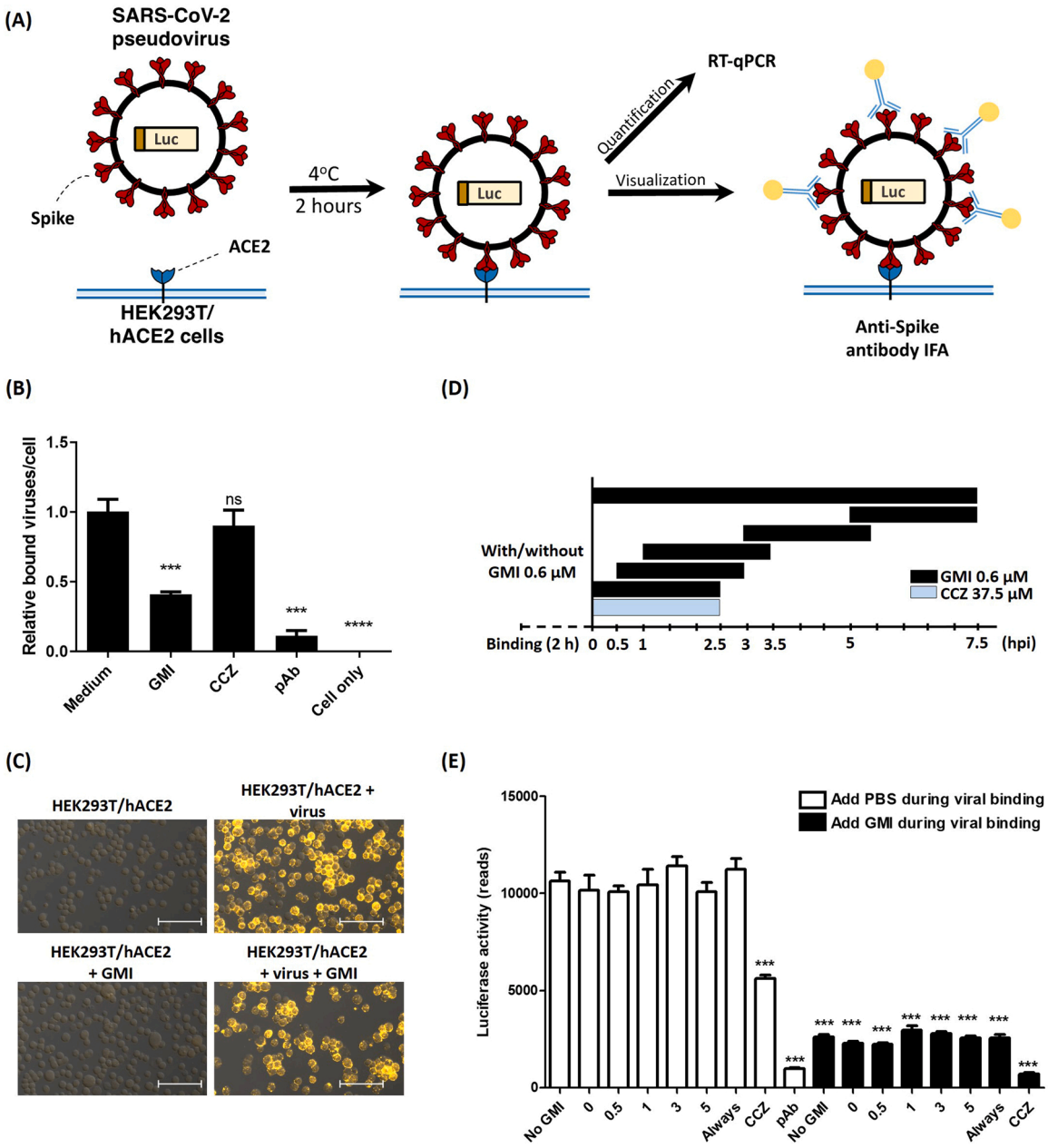

Fig. 2. GMI impedes the SARS-CoV-2 spike pseudotyped virus from binding to ACE2-bearing cells and inhibits viral infection. (A) Schematic design of viral binding assay. **(B)** HEK293T/hACE2 cells were exposed to spike pseudoviruses at 4 ℃ with GMI, CCZ, or polyclonal antiserum against SARS-CoV-2 (pAb) for 2 h. The virus-bound cells were collected after intensively washing by PBS and subjected for RT-qPCR using primers specific to actin gene and pLAS2 vector. In parallel, a viral binding assay was performed but here the bound spike pseudotyped viruses were visualized by **(C)** immunofluorescence staining with an antibody specific to the spike protein. **(D)** A schematic design described an assay of adding GMI/CCZ at different time points. **(E)** Following experimental design in (D), HEK293T/hACE2 cells were at first exposed to Spike pseudotyped viruses carrying luciferase and with or without GMI at 4 ℃ for 2 h to allow viral binding. After washing the viruses-bound cells with PBS to remove unbound viruses, the cells were incubated for 48 h at 37 ℃ for viral infection. Meanwhile, GMI were added at early (0–2.5 h, 0.5–3 h), middle (1–3.5 h), or late (3–5.5 h and 5–7.5 h) time points post-infection. Two conditions that cells were continuously treated with GMI or PBS after being seeded back to 37 °C were shown as "Always" and "No GMI". The reported fusion inhibitor CCZ was added to the cells at early time point (0–2.5 h) as indicator for fusion ability. The inhibition effect of spike antiserum was also examined as indicator for binding ability during binding assay. For whole experiment the concentration of each inhibitor was as following: GMI 0.6 μM; CCZ 37.5 μM; pAb 1:100 dilutions. The data are shown as the means ± SDs (error bars). Student's *t* test was used, $P < 0.05$ indicates a statistically significant difference whereas $P > 0.05$ implies the opposite; * ** $P < 0.001$, * ** * $P < 0.0001$, ns $P > 0.05$. The scale bar in the figures represents 100 μm.

150 mM sodium chloride, 1% sodium deoxycholate and proteinase inhibitor (Roche)). Lysates were subjected for sonication and then centrifugation before being denatured for 10 min at 95 °C in Laemmli buffer. SDS-polyacrylamide gels were used to separate the proteins prior to transferring onto polyvinylidene difluoride (PVDF) membranes (Bio-Rad). After blocking in 3% milk in PBS with 0.05% Tween 20, the blotted membranes were incubated with the indicated first/second antibodies. Visualization was performed with a chemiluminescent reagent (Pierce) and the signal intensity was evaluated with ImageJ software.

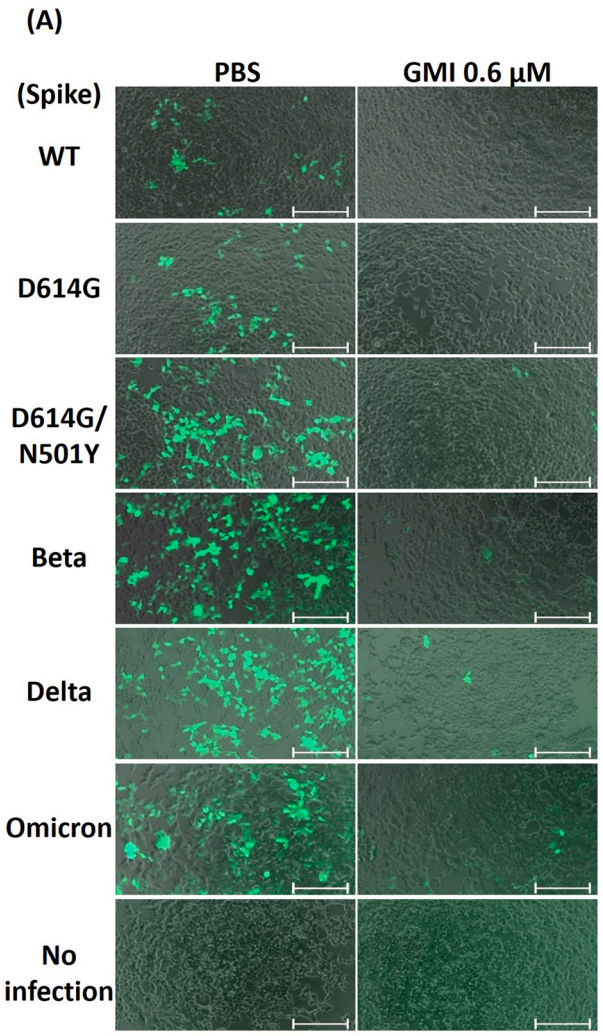

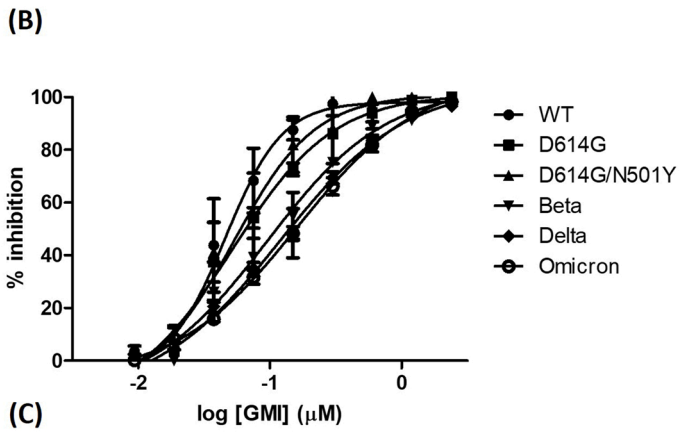

(C)

Spike	WT	D614G	D614G/ N501Y	Beta	Delta	Omicron
EC50 GMI (μM)	0.0462	0.0521	0.0535	0.0957	0.1208	0.1609

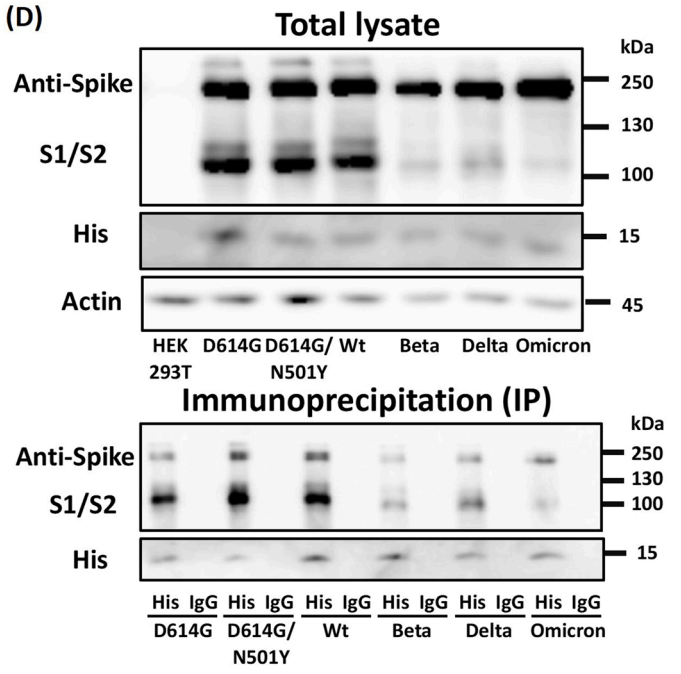

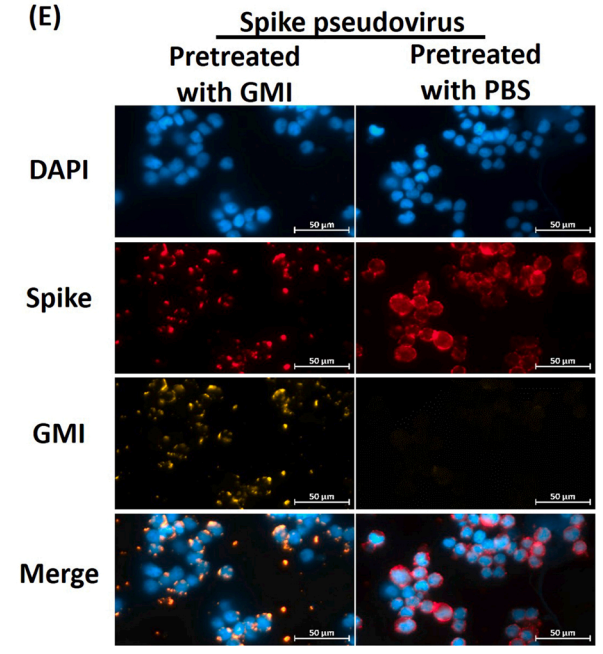

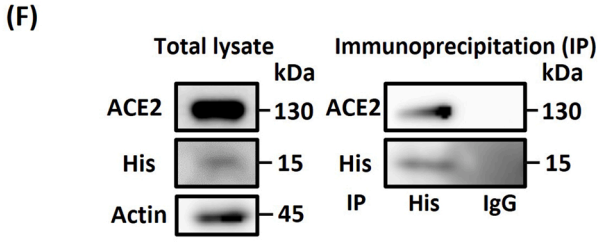

(caption on next page)

Fig. 3. Efficacy of GMI against SARS-CoV-2 variants. (A) SARS-CoV-2 Spike pseudotyped viruses carrying a GFP gene and packaged by SARS-CoV-2 Spike protein from wildtype virus, spike with D614G or D614G/N501Y mutation and spike from Beta, Delta, and Omicron variants were generated and hence applied for HEK293T/hACE2 infection with or without the treatment of 0.6 μM GMI. 48 h post-infection, the infectivity was visualized by using a fluorescence microscope. **(B)** The inhibition against SARS-Cov-2 pseudovirus infection by using various concentrations of GMI; **(C)** EC50 of GMI against Spike pseudotyped virus carrying different spike mutations/variants were shown. **(D)** HEK293T cells were transfected with a plasmid encoding the indicated spike protein. Cells were replenished with a fresh medium at 24 h post-transfection. 72 h post-transfection, the cells were treated with 1.2 μM GMI at 37 °C degree for 2 h. After extensive washing with PBS, the cells were collected, and the lysates were subjected to an immunoprecipitation assay. Here the total lysate and the immunoprecipitation results collected from cells transfected with different spike mutations or variants were shown. **(E)** Spike pseudovirions were treated with 1.2 μM GMI at 4 ℃ for 2 h and then were pelleted down by gradient centrifugation. The viruses were resuspended in culture medium and applied for binding assay in combination with immunofluorescence staining to visualize the cell-bound viruses by a rabbit antiserum against spike protein together with a Cy5-conjugated secondary antibody (red color). The samples were also double stained by using a mouse monoclonal antibody against His tag in combination with a Cy3-conjugated secondary antibody (yellow color). DAPI (blue color) was applied for visualizing the cell nuclei. **(F)** An immunoprecipitation assay similar as (D) to investigate the interaction between ACE2 and GMI was conducted. The scale bar in the (A) represents 100 μm and in (E) represents 50 μm.

2.11. Statistical analysis and software

The *P* values for significance testing between the control and the sample were analyzed by unpaired Student's *t* tests with the help of GraphPad Prism 5. All experiments were conducted at least three times and data were shown as mean ± SD. $P < 0.05$ indicates a statistically significant difference whereas $P > 0.05$ implies the opposite. In figures, *P* values are noted as following: * $P < 0.05$, * * $P < 0.01$, * ** $P < 0.001$, * ** * $P < 0.0001$, ns $P > 0.05$.

3. Results

3.1. GMI exhibits favorable antiviral effects against spike pseudotyped virus infection in different cell lines

We first explored the antiviral efficacy of GMI against lentiviral-based spike pseudotyped viruses carrying the spike D614G/N501Y mutation commonly observed in the current SARS-CoV-2 variants [10]. By using spike-pseudotyped viruses containing a luciferase gene to expose with different cell lines, we found that GMI inhibited the spike-pseudotyped virus infection with 50% effective concentration (EC50) at 0.077 μM in HEK293T/hACE2 and 0.013 μM in A549/hACE2 (Fig. 1 A). Since the pseudotyped viruses examined here only infect the cells without having further viral replication, the inhibition effects offered by GMI should be due to either the reduction of viral binding or the entry to ACE2-bearing cells thereafter. To simulate the vaccination protection of current COVID-19 vaccines, we used a polyclonal antiserum against wildtype spike protein which could block viral binding (Supplementary Fig. S1). CCZ, a reported chemical that could block SARS-CoV-2 fusion [38], was also examined (Fig. 1B). Meanwhile, GMI showed 50% cytotoxicity concentration (CC50) at more than 2 μM for both cell types whereas CCZ had high cell cytotoxicity to HEK293T cells with CC50 value at 42.03 μM, which was 3-fold less concentrated than IC50 (Fig. 1). We did not observe the significant cytotoxicity of the cells treated with antiserum against SARS-CoV-2 although it can only achieve efficient inhibition while using higher than 25-fold dilution of the original antiserum (Supplementary Fig. S1). The safety tests of genetic, embryo-fetal, and oral toxicity tests in rats of GMI had also been recently reported [39]. Overall, these data showed that GMI could become a good candidate for inhibiting SARS-CoV-2 infection.

3.2. GMI blocks the spike-bearing virus binding to ACE2-expressing cells

To dissect whether GMI interferes with viral attachment, we performed a binding assay by exposing HEK293T/hACE2 cells to spike-pseudotyped virus with the presence of GMI as mentioned in methods and the relative numbers of viruses bound to each cell were quantified by RT-qPCR (Fig. 2 A). A fusion inhibitor, CCZ and a polyclonal anti-spike antiserum were also included in the same tests. Our results showed that both spike antibody and GMI can inhibit the spike-pseudotyped viruses binding to HEK293T/hACE2 cells whereas CCZ only had minor effects (Fig. 2B). The inhibitory effect of GMI on the binding between spike-pseudotyped virus and the cells was also validated by immunostaining (Fig. 2 C). To further elucidate whether GMI also influences viral entry, a time of addition/removal assay was performed. In the same experiment, polyclonal anti-spike antiserum and CCZ were also included. The binding assay between spike-pseudoviruses and HEK293T/hACE2 cells was performed for 2 h at 4 °C with or without the indicated inhibitors. After removing the unbound viruses, the virus-bound cells were moved from 4 °C to 37 °C for evaluating the internationalization of the viruses into the cells. GMI was inoculated at different time points for 2.5 h to decide the possible timing of viral entry (Fig. 2D). In the same vein of the binding assay shown in Fig. 2 A, treatment of GMI only at virus-cell binding step reduces 75% of the infectivity thereafter (Fig. 2E). Surprisingly, we did not observe any further inhibition effect of GMI on the viruses-bound cells regardless of the addition of GMI treatment at the binding step. On the other hand, early treatment of the fusion inhibitor CCZ could further inhibit viral entry of the virus-bound cells even with or without GMI treatment during binding (Fig. 2E). In summary, these results indicated that GMI could be a promising candidate for the prevention of SARS-CoV-2 infection through inhibiting the spike-bearing virus binding to the hACE2-expressing cells. It is also important to address that this inhibition seemed to not require the downregulation of ACE2 protein as reported previously since whole viral binding procedures were performed on ice [34].

3.3. GMI has broad-spectrum antiviral effects against SARS-CoV-2 spike variants by direct binding to the spike protein

The emerging concern of COVID-19 pandemic is the rapid mutation in spike protein from different SARS-CoV-2 variants and clearly these variants are more infectious with less susceptibility to vaccine-mediated immune protection [8–10, 40]. We therefore generated pseudotyped lentivirus carrying a GFP gene and harboring SARS-CoV-2 spike protein derived from different clinical strains or with mutations. Our results indicated that GMI treatment at infection could efficiently inhibit the infection of pseudotyped viruses carrying different spike proteins, including the currently emerging Delta and Omicron strains (Fig. 3A-C). Meanwhile, the pseudotyped viruses harboring different spike variants showed susceptibility to GMI with EC50 values ranging from 0.0462 to 0.1609 μM. Interestingly, the previous pandemic Beta strain and the currently pandemic strain Delta and Omicron required 2- to 3.5-fold higher concentration of GMI than wildtype strain and the difference seems corresponding to the reported transmission ability (Fig. 3B and C). This could be explained by the increasing affinity with ACE2 and the enhanced fusion ability to the target cells gained by the mutations of the spike protein in these pandemic strains [40–44]. We therefore wish to investigate whether GMI could directly bind to the spike protein or ACE2 protein to inhibit viral binding. Here we performed an immunoprecipitation assay and validated that GMI binds to all the tested spike proteins with high efficiency (Fig. 3D). We also confirmed that GMI co-localized with spike pseudotyped viruses through viral binding assay with HEK293/hACE2 in combination with immunofluorescence staining

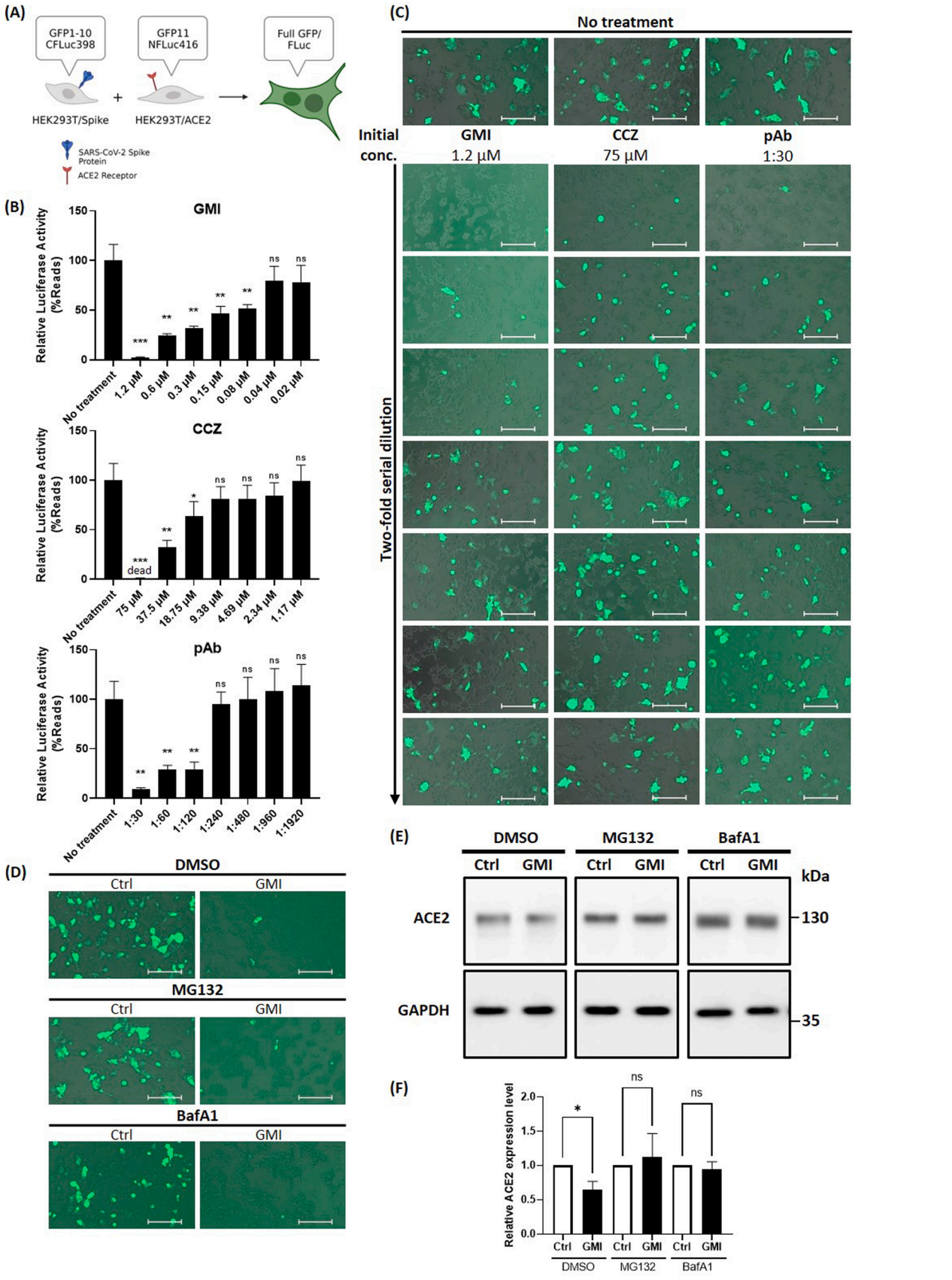

(caption on next page)

Fig. 4. GMI inhibits spike-mediated syncytia formation even without ACE2 degradation. (A) Schematic design of cell-cell fusion assay (Created with BioRender.com). HEK293T/Spike was transfected with GFP1–10 and CFLuc398 (effector cells) while HEK293T/ACE2 was transfected with GFP11 and NFLuc416 (target cells) so that only fused cells will produce GFP and firefly luciferase signals. 24 h post-transfection, effector and target cells were mixed (1:1 ratio) and co-plated for 24 h before cell-cell fusion rate was documented by luminometer **(B)** and fluorescence microscopy **(C-D)**. **(B-C)** Mixed cells were co-cultured with PBS (no treatment control) or GMI, CCZ, polyclonal antibody at different concentrations (2-fold serial dilution, initial concentrations are as indicated). **(D-E)** 24 h post transfection, target cells were pretreated with DMSO, MG132 (10 μM), BafA1 (20 nM) for 30 min **(D)** Pretreated cells were co-cultured with transfected effector cells and continuous treatment of DMSO, MG132 (10 μM), BafA1 (20 nM) with/without the addition of 0.6 μM GMI. **(E)** Pretreated target cells alone were continuingly treated with DMSO, MG132 (10 μM), BafA1 (20 nM) with/without the addition of 0.6 μM GMI for 24 h before cells were collected for ACE2 Western blotting. The data are shown as the means ± SDs (error bars). Student's *t* test was used, $P < 0.05$ indicates a statistically significant difference whereas $P > 0.05$ implies the opposite; * $P < 0.05$, * * $P < 0.01$, * ** $P < 0.001$, ns $P > 0.05$. The scale bar in the figures represents 200 μm.

(Fig. 3E). We applied rabbit polyclonal anti-spike antiserum for all the experiments since several monoclonal antibodies against spike protein might not recognize all the spike variants. Indeed, we observed that the rabbit antiserum we applied here had weaker affinity against spike variants Beta, Delta, and Omicron, but this did not influence the immunoprecipitation assay. Our data suggested that GMI could also bind to ACE2 protein (Fig. 3 F). Overall, these results indicate that GMI could block the infection of spike pseudotyped virus bearing different spike variants by directly targeting the spike protein, which leads to the inefficient viral binding to the host cells and ultimately results in the inhibition of SARS-CoV-2 infection.

3.4. GMI has a broad-spectrum inhibiting ability against SARS-CoV-2 spike-mediated cell-cell fusion

Enveloped viruses can achieve viral transmission in cell culture system and in the tissue via cell-free particles or directly by cell-cell contact [45–50]. Importantly, the model of cell-to-cell transmission through spike and ACE2 fusion had been reported with higher efficiency for viral transmission in SARS-CoV-2-infected cells as well as with high resistance to antibody-mediated protection [45]. Meanwhile, ACE2-spike interaction can ultimately lead to strong cell syncytia and severe pathological consequence in SARS-CoV-2 patients [50–53]. To evaluate the effects of GMI on spike-medicated cell fusion, we established a dual split GFP/firefly luciferase system that allows us to evaluate the fusion efficacy only after the fusion happens (Fig. 4 A). By using the split GFP as monitor, our data showed that GMI can efficiently impede ACE2-spike-mediated cell fusion at dose-dependent manner. Strikingly, the possible fusion-blocking candidate, CCZ, showed the weakest inhibition effect. CCZ at 75 μM induced major cell death. Although CCZ at the concentration of 37.5 μM, which is closed to CC50, could efficiently block cell-free virus infection, it only gained minor reduction in cell-cell fusion (Fig. 1B). By using the split luciferase system, our experimental model showed that GMI could achieve 50% inhibition of ACE2-spike-mediated fusion even at 0.075 μM corresponding to the determined IC50 of the cell-free virus model (Figs. 4B, 4 C and 1 A). Meanwhile, we found that polyclonal anti-spike antiserum could also inhibit cell fusion mediated by ACE2-spike interaction as reported previously [45] although extremely high concentration was required (Figs. 4B and 4 C). As the Spike antibody has high molecular weight (more than 150 kDa), its neutralization effects against these cell-to-cell fusion in tissues where cells are tightly attached to each other are still controversial [45]. In contrast, GMI, which is a very small protein with only 12 kDa in size, has much higher potency in penetrating into the tissues. In comparison to the ability of these inhibitors toward cell-free viruses (Fig. 1), our results showed that GMI exhibits superior inhibition effects against SARS-CoV-2 at both cell-free virus infection and cell-cell fusion. We also confirmed that GMI could exhibit strong inhibition effects on spike-ACE2-mediated cell fusion without the requirement of ACE2 degradation as previous report (Fig. 4D and E) [34].

The high mutation rates of SARS-CoV-2 would lead to the emergence of mutations acquiring immune escape properties from neutralization antibodies. Many of these spike variants also showed stronger potency in causing cell-cell fusion regulated by the interaction between spike protein and ACE2. We here showed that GMI could efficiently impede cell-cell fusion mediated by the spike protein derived from different SARS-CoV-2 strains, even better than CCZ and polyclonal antibody (Fig. 5 A, B and C).

3.5. Combination treatment using GMI further enhances inhibition against spike-mediated cell-cell fusion

In the subsequent experiment, we wished to further augment the inhibitory effect of GMI against syncytia formation by combining GMI with several existing cell-cell fusion inhibitors. Similar assay as depicted in Fig. 4 A was applied using HEK293T/Spike as effector cells and HEK293T/ACE2 as target cells so that only fused cells would emit GFP and firefly luciferase signals. PBS was added during the 2-day co-plating period as no treatment control while 37.5 μM CCZ, 100-fold diluted spike polyclonal antibody and their combination with 0.6 μM GMI treatment were also used in the same panel of experiment. Although GMI treatment alone at 0.6 μM could already decrease fusion rate substantially, our results showed that this inhibition could be additionally enhanced when combined with the investigated inhibitors (Fig. 6 A, B). Moreover, this accumulated effect also implied that GMI might have a different pathway to prevent syncytia formation compared to CCZ and spike-antibody. Taken together, GMI should be considered as a potential candidate to increase the treatment and prevention efficacy in combination therapy with other reagents.

4. Discussion

As the rapid mutations acquired by many SARS-CoV-2 variants (especially the prevalent ones such as Omicron and its subvariants) have been leading to mass resistance against currently available vaccines [5,8,10,54]. Increasing concern and attention towards broad-spectrum prevention and treatment strategies are being recorded. Since the severity of COVID-19 is positively correlated to the viral load observed in the infected patients, the antivirals that can lead to the inhibition of viral binding, entry, replication, or release step, would be beneficial to inhibit the pathological effects after viral infection and transmission [55,56]. Currently, the Emergency Use Authorization antiviral drugs against SARS-CoV-2, including Paxlovid and Molnupiravir are both inhibiting SARS-CoV-2 specifically at viral replication step [19,21,22,24] whereas the authorized new antivirals against SARS-CoV-2 at binding, entry, and transmission are currently not accessible. Hence, the new antiviral candidates should be urgently investigated, especially the antivirals targeting beyond viral replication since the combinational drug therapy against fast mutating RNA viruses could be a reasonable strategy to prevent drug-resistant viruses. Nevertheless, it is frustrating that the development of new drugs is time- and money-consuming and their safety for individual usage requires further tests. Regarding the rapid evolution of SARS-CoV-2, the fast but assuring safe antiviral candidates should be prioritized.

On the other hand, several FDA-approved drugs had been repurposed for combating COVID-19 with acceptable side effects in human [57–62]; however, only some of which were reported with beneficial effects in hospitalized COVID-19 patients. For example, Remdesivir, a nucleoside drug against a variety of viruses, helps to shorten the recovery time of hospitalized COVID-19 patients [23]. Meanwhile, Baricitinib, a Janus

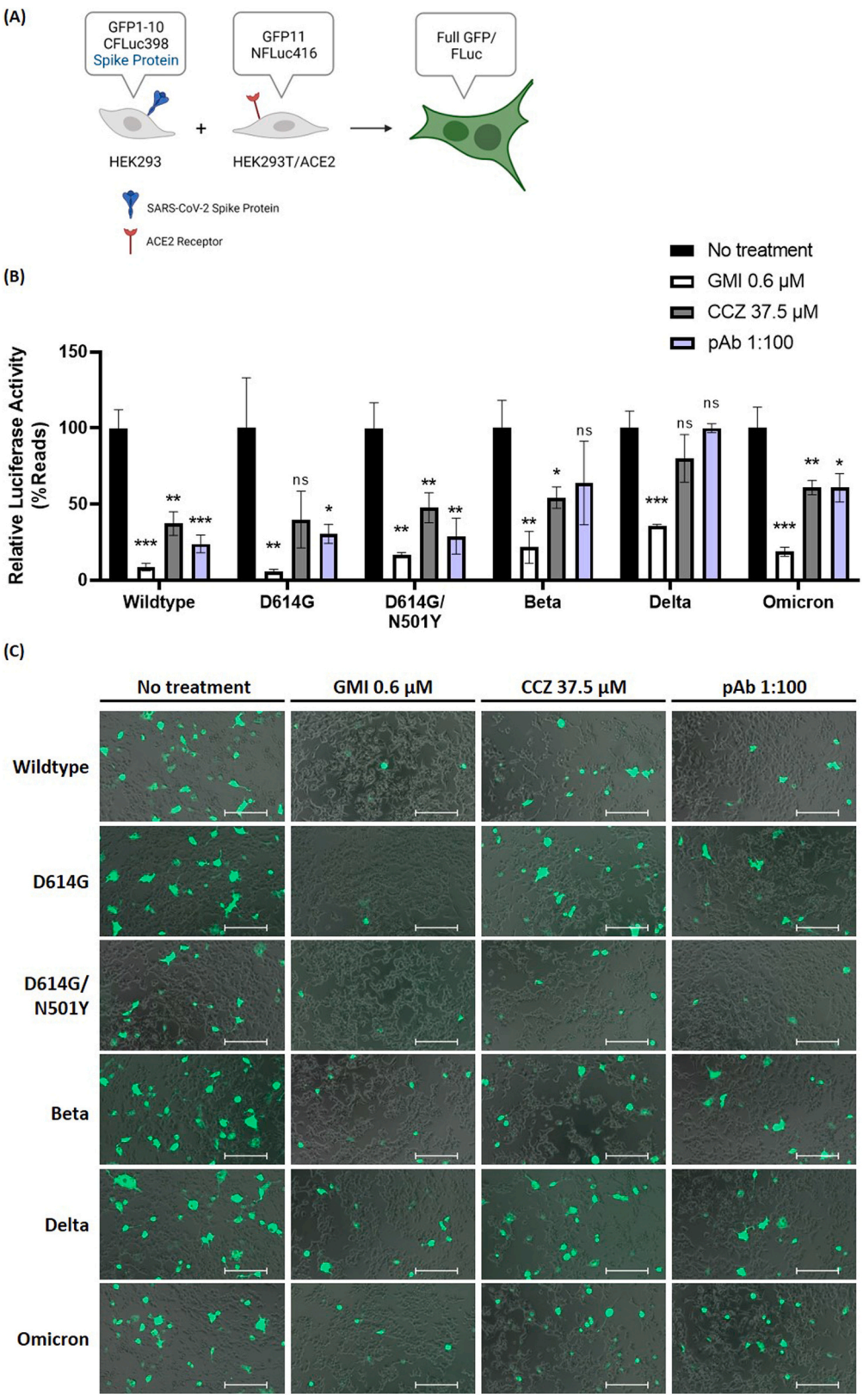

Fig. 5. GMI strongly reduces syncytia formation between ACE2-bearing cells and cells overexpressing mutated or different variants' spike proteins. (A) Schematic design of cell-cell fusion assay (Created with BioRender.com). HEK293 was transfected with different spike plasmids, GFP1–10 and CFLuc398 (effector cells) while HEK293T/ACE2 was transfected with GFP11 and NFLuc416 (target cells) so that only fused cells will produce GFP and firefly luciferase signals. 24 h post-transfection, effector and target cells were mixed (1:1 ratio) and co-cultured with PBS (no treatment control) or with 0.6 μM GMI, 37.5 μM CCZ, 100-fold diluted polyclonal antibody. Cell-cell fusion rate was documented by a luminometer at 12 h **(B)** and by a fluorescence microscopy at 24 h **(C)**. Student's *t* test was used, $P < 0.05$ indicates a statistically significant difference whereas $P > 0.05$ implies the opposite; * $P < 0.05$, * * $P < 0.01$, * ** $P < 0.001$, ns $P > 0.05$. The scale bar in the figures represents 200 μm.

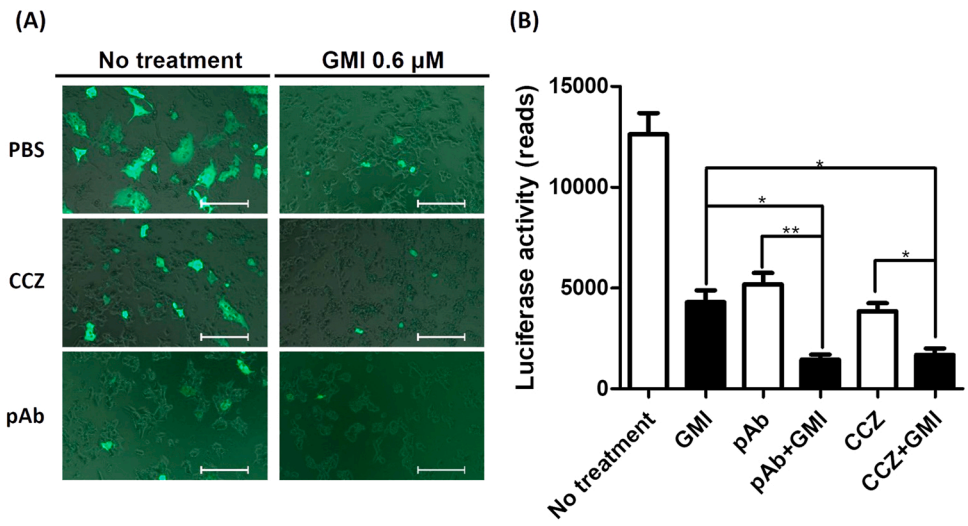

Fig. 6. Inhibitory effect of GMI against spike-mediated cell-cell fusion is enhanced when combined with other inhibitors. HEK293T/Spike was transfected with GFP1–10 and CFLuc398 (effector cells) while HEK293T/ACE2 was transfected with GFP11 and NFLuc416 (target cells) so that only fused cells will produce GFP and firefly luciferase signals. 24 h post-transfection, effector and target cells were mixed (1:1 ratio) and co-plated with the indicated agents for 24 h before cell-cell fusion rate was documented by **(A)** fluorescence microscopy and **(B)** luminometer. Student's *t* test was used, $P < 0.05$ indicates a statistically significant difference whereas $P > 0.05$ implies the opposite; * $P < 0.05$, * * $P < 0.01$, * ** $P < 0.001$, ns $P > 0.05$. The scale bar in the figures represents 200 μm.

Kinase inhibitor could speed up viral clearance of COVID-19 patients by reducing cytokine release [63]. Nevertheless, these drugs could only provide moderate or minor clinical benefits and their side effects should be considered; hence they are mainly applied in severe COVID-19 patients. Many of these repurposed drugs are mostly targeting viral replication or reducing cytokine storms whereas the available drug candidates that can be applied for impeding viral entry step required further investigation. Additionally, the neutralizing antibodies against SARS-CoV-2 acquired after vaccination should be considered as the best strategy for combating viral binding and entry steps. Moreover, the rapid emergence of SARS-CoV-2 variants escaping from protection implies the need for broad-spectrum antivirals that supplement the inefficient effects of neutralizing antibody.

In our previous publication, GMI has been reported to trigger ACE2 degradation through proteasome and lysosome pathways [34]. However, in this study, we found that GMI blocked SARS-CoV-2 cell-to-cell fusion independently to such pathways. Therefore, additionally possible cell signaling related to the inhibitory effects of GMI against SARS-CoV-2 syncytia formation should be investigated. The relationship between GMI and human body immunity is also noteworthy as it has been mentioned in various articles. GMI could restrict MDSC expansion to induce the proliferation of cytotoxic T cells [64]. In addition, GMI has been shown to have similar protein sequence and structure in comparison with Lingzhi 8 (LZ8) from *Ganoderma microsporum* . LZ-8 could increase mouse splenic mononuclear cells, human peripheral blood lymphocytes, PBMC, and the expression levels of IFN-γ, IL-2, IL-1β, TNF-α [65,66]. Hence, further experiments and *in vivo* model should be performed to elucidate the impacts of GMI on COVID-19 patient immunity.

5. Conclusions

Here our study validated that the fungal protein, GMI, behaves as a broad-spectrum antiviral agent against SARS-CoV-2 carrying different spike mutations. GMI is an FDA-approved dietary ingredient with validated low toxicity in genome stability, embryo development, and biosafety in animals, and we discovered its antiviral effects against SARS-CoV-2. In our previous study, we showed that GMI functions as a potential antiviral candidate against SARS-CoV-2 infection through the downregulation of ACE2 expression level in the host cells. Here, we provide the detailed pathway of how GMI blocks SARS-CoV-2 infection by not only direct blockage of viral binding, but also thereafter impeding cell-to-cell-mediated fusion caused by ACE2-spike interaction, which could lead to severe pathological effects. Importantly, we observed that GMI inhibits SARS-CoV-2 infection and cell-cell fusion without the requirement of downregulating ACE2 expression level, which indicates that GMI could be considered as a therapeutic candidate for SARS-CoV-2 infection.

Taken together, our results suggest that GMI is a promising candidate to inhibit the infection by different SARS-CoV-2 variants as well as to prevent the possible pathological consequences caused by syncytia formation caused after infection.

Authorship contribution statement

H.-P T. Ho, D.-N K. Vo, J.-N. Hung, Y.-H. Chiu and M.-H. Tsai performed experiments; H.-P T. Ho, D.-N K. Vo, T.-Y. Lin, and M.-H. Tsai edited manuscript and analyzed data. M.-H. Tsai designed research, providing conception, and wrote the manuscript. All of authors approved final version of manuscript.

Conflict of interest statement

The authors declare that they have no known competing financial interests or personal relationships that could have appeared to influence the work reported in this paper.

Data availability

Data will be made available on request.

Acknowledgements

The authors would like to express gratitude towards Dr. R.-S. Hseu (NTU, Taiwan) for providing the purified GMI. Lentiviral vectors and reagents were gratefully received from the National RNAi Core facility at Academia Sinica in Taiwan. This work was funded by the Ministry of Science and Technology (MOST111–2636-B-A49–003 and MOST111–2321-B-A49–007) and Yen Tjing Ling Medical Foundation (CI-110–12).

Appendix A. Supporting information

Supplementary data associated with this article can be found in the online version at doi:10.1016/j.biopha.2022.113766.

References

[1] W.H.O., Coronavirus (COVID-19) Dashboard., https://covid19.who.int/ (2022).

[2] A.G. Harrison, T. Lin, P. Wang, Mechanisms of SARS-CoV-2 transmission and pathogenesis, Trends Immunol. 41 (12) (2020) 1100–1115.

[3] D.E. Gordon, G.M. Jang, M. Bouhaddou, J. Xu, K. Obernier, K.M. White, M. J. O'Meara, V.V. Rezelj, J.Z. Guo, D.L. Swaney, T.A. Tummino, R. Huttenhain, R. M. Kaake, A.L. Richards, B. Tutuncuoglu, H. Foussard, J. Batra, K. Haas, M. Modak, M. Kim, P. Haas, B.J. Polacco, H. Braberg, J.M. Fabius, M. Eckhardt, M. Soucheray, M.J. Bennett, M. Cakir, M.J. McGregor, Q. Li, B. Meyer, F. Roesch, T. Vallet, A. Mac Kain, L. Miorin, E. Moreno, Z.Z.C. Naing, Y. Zhou, S. Peng, Y. Shi, Z. Zhang, W. Shen, I.T. Kirby, J.E. Melnyk, J.S. Chorba, K. Lou, S.A. Dai, I. Barrio-Hernandez, D. Memon, C. Hernandez-Armenta, J. Lyu, C.J.P. Mathy, T. Perica, K.B. Pilla, S. J. Ganesan, D.J. Saltzberg, R. Rakesh, X. Liu, S.B. Rosenthal, L. Calviello, S. Venkataramanan, J. Liboy-Lugo, Y. Lin, X.P. Huang, Y. Liu, S.A. Wankowicz, M. Bohn, M. Safari, F.S. Ugur, C. Koh, N.S. Savar, Q.D. Tran, D. Shengjuler, S. J. Fletcher, M.C. O'Neal, Y. Cai, J.C.J. Chang, D.J. Broadhurst, S. Klippsten, P. P. Sharp, N.A. Wenzell, D. Kuzuoglu-Ozturk, H.Y. Wang, R. Trenker, J.M. Young, D. A. Cavero, J. Hiatt, T.L. Roth, U. Rathore, A. Subramanian, J. Noack, M. Hubert, R. M. Stroud, A.D. Frankel, O.S. Rosenberg, K.A. Verba, D.A. Agard, M. Ott, M. Emerman, N. Jura, M. von Zastrow, E. Verdin, A. Ashworth, O. Schwartz, C. d'Enfert, S. Mukherjee, M. Jacobson, H.S. Malik, D.G. Fujimori, T. Ideker, C. S. Craik, S.N. Floor, J.S. Fraser, J.D. Gross, A. Sali, B.L. Roth, D. Ruggero, J. Taunton, T. Kortemme, P. Beltrao, M. Vignuzzi, A. Garcia-Sastre, K.M. Shokat, B. K. Shoichet, N.J. Krogan, A SARS-CoV-2 protein interaction map reveals targets for drug repurposing, Nature 583 (7816) (2020) 459–468.

[4] A.C. Walls, Y.J. Park, M.A. Tortorici, A. Wall, A.T. McGuire, D. Veesler, Structure, function, and antigenicity of the SARS-CoV-2 spike glycoprotein, Cell 181 (2) (2020) 281–292, e6.

[5] J.S. Tregoning, K.E. Flight, S.L. Higham, Z. Wang, B.F. Pierce, Progress of the COVID-19 vaccine effort: viruses, vaccines and variants versus efficacy, effectiveness and escape, Nat. Rev. Immunol. 21 (10) (2021) 626–636.

[6] J. Li, S. Lai, G.F. Gao, W. Shi, The emergence, genomic diversity and global spread of SARS-CoV-2, Nature 600 (7889) (2021) 408–418.

[7] C. Liu, H.M. Ginn, W. Dejnirattisai, P. Supasa, B. Wang, A. Tuekprakhon, R. Nutalai, D. Zhou, A.J. Mentzer, Y. Zhao, H.M.E. Duyvesteyn, C. Lopez-Camacho, J. Slon-Campos, T.S. Walter, D. Skelly, S.A. Johnson, T.G. Ritter, C. Mason, S. A. Costa Clemens, F. Gomes Naveca, V. Nascimento, F. Nascimento, C. Fernandes da Costa, P.C. Resende, A. Pauvolid-Correa, M.M. Siqueira, C. Dold, N. Temperton, T. Dong, A.J. Pollard, J.C. Knight, D. Crook, T. Lambe, E. Clutterbuck, S. Bibi, A. Flaxman, M. Bittaye, S. Belij-Rammerstorfer, S.C. Gilbert, T. Malik, M. W. Carroll, P. Klenerman, E. Barnes, S.J. Dunachie, V. Baillie, N. Serafin, Z. Ditse, K. Da Silva, N.G. Paterson, M.A. Williams, D.R. Hall, S. Madhi, M.C. Nunes, P. Goulder, E.E. Fry, J. Mongkolsapaya, J. Ren, D.I. Stuart, G.R. Screaton, Reduced neutralization of SARS-CoV-2 B.1.617 by vaccine and convalescent serum, Cell 184 (16) (2021) 4220–4236, e13.

[8] B.J. Willett, J. Grove, O.A. MacLean, C. Wilkie, G. De Lorenzo, W. Furnon, D. Cantoni, S. Scott, N. Logan, S. Ashraf, M. Manali, A. Szemiel, V. Cowton, E. Vink, W.T. Harvey, C. Davis, P. Asamaphan, K. Smollett, L. Tong, R. Orton, J. Hughes, P. Holland, V. Silva, D.J. Pascall, K. Puxty, A. da Silva Filipe, G. Yebra, S. Shaaban, M.T.G. Holden, R.M. Pinto, R. Gunson, K. Templeton, P.R. Murcia, A.H. Patel, P. Klenerman, S. Dunachie, J. Haughney, D.L. Robertson, M. Palmarini, S. Ray, E. C. Thomson, SARS-CoV-2 Omicron is an immune escape variant with an altered cell entry pathway, Nat. Microbiol. (2022).

[9] D. Tian, Y. Sun, J. Zhou, Q. Ye, The global epidemic of the SARS-CoV-2 delta variant, key spike mutations and immune escape, Front Immunol. 12 (2021), 751778.

[10] W.T. Harvey, A.M. Carabelli, B. Jackson, R.K. Gupta, E.C. Thomson, E.M. Harrison, C. Ludden, R. Reeve, A. Rambaut, S.J. Peacock, D.L. Robertson, SARS-CoV-2 variants, spike mutations and immune escape, Nat. Rev. Microbiol. 19 (7) (2021) 409–424.

[11] A. Bess, F. Berglind, S. Mukhopadhyay, M. Brylinski, N. Griggs, T. Cho, C. Galliano, K.M. Wasan, Artificial intelligence for the discovery of novel antimicrobial agents for emerging infectious diseases, Drug Discov. Today 27 (4) (2022) 1099–1107.

[12] T. Xu, W. Zheng, R. Huang, High-throughput screening assays for SARS-CoV-2 drug development: current status and future directions, Drug Discov. Today 26 (10) (2021) 2439–2444.

[13] S. Bibi, M.S. Khan, S.A. El-Kafrawy, T.A. Alandijany, M.M. El-Daly, Q. Yousafi, D. Fatima, A.A. Faizo, L.H. Bajrai, E.I. Azhar, Virtual screening and molecular dynamics simulation analysis of Forsythoside A as a plant-derived inhibitor of SARS-CoV-2 3CLpro, Saudi pharmaceutical journal: SPJ: the official publication of the Saudi Pharmaceutical, Society 30 (7) (2022) 979–1002.

[14] R. Wang, P. Stephen, Y. Tao, W. Zhang, S.X. Lin, Human endeavor for anti-SARS-CoV-2 pharmacotherapy: a major strategy to fight the pandemic, Biomed. Pharmacother. = Biomedecine Pharmacother. 137 (2021), 111232.

[15] M. Kumari, R.M. Lu, M.C. Li, J.L. Huang, F.F. Hsu, S.H. Ko, F.Y. Ke, S.C. Su, K. H. Liang, J.P. Yuan, H.L. Chiang, C.P. Sun, I.J. Lee, W.S. Li, H.P. Hsieh, M.H. Tao, H.C. Wu, A critical overview of current progress for COVID-19: development of vaccines, antiviral drugs, and therapeutic antibodies, J. Biomed. Sci. 29 (1) (2022) 68.

[16] S. Barsi, H. Papp, A. Valdeolivas, D.J. Tóth, A. Kuczmog, M. Madai, L. Hunyady, P. Várnai, J. Saez-Rodriguez, F. Jakab, B. Szalai, Computational drug repurposing against SARS-CoV-2 reveals plasma membrane cholesterol depletion as key factor of antiviral drug activity, PLoS Comput. Biol. 18 (4) (2022), e1010021.

[17] S. Bibi, M.M. Hasan, Y.B. Wang, S.P. Papadakos, H. Yu, Cordycepin as a promising inhibitor of SARS-CoV-2 RNA dependent RNA polymerase (RdRp), Curr. Med. Chem. 29 (1) (2022) 152–162.

[18] D. Dey, R. Hossain, P. Biswas, P. Paul, M.A. Islam, T.I. Ema, B.K. Gain, M.M. Hasan, S. Bibi, M.T. Islam, M.A. Rahman, B. Kim, Amentoflavone derivatives significantly act towards the main protease (3CL(PRO)/M(PRO)) of SARS-CoV-2: in silico admet profiling, molecular docking, molecular dynamics simulation, network pharmacology, Mol. Divers. (2022) 1–15.

[19] D.R. Owen, C.M.N. Allerton, A.S. Anderson, L. Aschenbrenner, M. Avery, S. Berritt, B. Boras, R.D. Cardin, A. Carlo, K.J. Coffman, A. Dantonio, L. Di, H. Eng, R. Ferre, K.S. Gajiwala, S.A. Gibson, S.E. Greasley, B.L. Hurst, E.P. Kadar, A.S. Kalgutkar, J. C. Lee, J. Lee, W. Liu, S.W. Mason, S. Noell, J.J. Novak, R.S. Obach, K. Ogilvie, N. C. Patel, M. Pettersson, D.K. Rai, M.R. Reese, M.F. Sammons, J.G. Sathish, R.S. P. Singh, C.M. Steppan, A.E. Stewart, J.B. Tuttle, L. Updyke, P.R. Verhoest, L. Wei, Q. Yang, Y. Zhu, An oral SARS-CoV-2 M(pro) inhibitor clinical candidate for the treatment of COVID-19, Science 374 (6575) (2021) 1586–1593.

[20] C.M. Chu, V.C. Cheng, I.F. Hung, M.M. Wong, K.H. Chan, K.S. Chan, R.Y. Kao, L. L. Poon, C.L. Wong, Y. Guan, J.S. Peiris, K.Y. Yuen, Role of lopinavir/ritonavir in the treatment of SARS: initial virological and clinical findings, Thorax 59 (3) (2004) 252–256.

[21] F. Kabinger, C. Stiller, J. Schmitzova, C. Dienemann, G. Kokic, H.S. Hillen, C. Hobartner, P. Cramer, Mechanism of molnupiravir-induced SARS-CoV-2 mutagenesis, Nat. Struct. Mol. Biol. 28 (9) (2021) 740–746.

[22] A. Jayk Bernal, M.M. Gomes da Silva, D.B. Musungaie, E. Kovalchuk, A. Gonzalez, V. Delos Reyes, A. Martín-Quirós, Y. Caraco, A. Williams-Diaz, M.L. Brown, J. Du, A. Pedley, C. Assaid, J. Strizki, J.A. Grobler, H.H. Shamsuddin, R. Tipping, H. Wan, A. Paschke, J.R. Butterton, M.G. Johnson, C. De, Anda, molnupiravir for oral treatment of covid-19 in nonhospitalized patients, N. Engl. J. Med. 386 (6) (2022) 509–520.

[23] J.H. Beigel, K.M. Tomashek, L.E. Dodd, A.K. Mehta, B.S. Zingman, A.C. Kalil, E. Hohmann, H.Y. Chu, A. Luetkemeyer, S. Kline, D. Lopez de Castilla, R. W. Finberg, K. Dierberg, V. Tapson, L. Hsieh, T.F. Patterson, R. Paredes, D. A. Sweeney, W.R. Short, G. Touloumi, D.C. Lye, N. Ohmagari, M.D. Oh, G.M. Ruiz-Palacios, T. Benfield, G. Fätkenheuer, M.G. Kortepeter, R.L. Atmar, C.B. Creech, J. Lundgren, A.G. Babiker, S. Pett, J.D. Neaton, T.H. Burgess, T. Bonnett, M. Green, M. Makowski, A. Osinusi, S. Nayak, H.C. Lane, Remdesivir for the treatment of Covid-19 - final report, N. Engl. J. Med. 383 (19) (2020) 1813–1826.

[24] J. Hammond, H. Leister-Tebbe, A. Gardner, P. Abreu, W. Bao, W. Wisemandle, M. Baniecki, V.M. Hendrick, B. Damle, A. Simón-Campos, R. Pypstra, J.M. Rusnak, Oral nirmatrelvir for high-risk, nonhospitalized adults with covid-19, N. Engl. J. Med. 386 (15) (2022) 1397–1408.

[25] P. Biswas, M.M. Hasan, D. Dey, A.C. Dos Santos Costa, S.A. Polash, S. Bibi, N. Ferdous, M.A. Kaium, M.D.H. Rahman, F.K. Jeet, S. Papadakos, K. Islam, M. S. Uddin, Candidate antiviral drugs for COVID-19 and their environmental implications: a comprehensive analysis, Environ. Sci. Pollut. Res. Int. 28 (42) (2021) 59570–59593.

[26] M.P. Manns, B. Maasoumy, Breakthroughs in hepatitis C research: from discovery to cure, Nat. Rev. Gastroenterol. Hepatol. (2022) 1–18.

[27] E. De, Clercq, The design of drugs for HIV and HCV, Nat. Rev. Drug Discov. 6 (12) (2007) 1001–1018.

[28] A. Glasgow, J. Glasgow, D. Limonta, P. Solomon, I. Lui, Y. Zhang, M.A. Nix, N. J. Rettko, S. Zha, R. Yamin, K. Kao, O.S. Rosenberg, J.V. Ravetch, A.P. Wiita, K. K. Leung, S.A. Lim, X.X. Zhou, T.C. Hobman, T. Kortemme, J.A. Wells, Engineered ACE2 receptor traps potently neutralize SARS-CoV-2, Proc. Natl. Acad. Sci. USA 117 (45) (2020) 28046–28055.

[29] N. Zamorano Cuervo, N. Grandvaux, ACE2: Evidence of role as entry receptor for SARS-CoV-2 and implications in comorbidities, eLife 9 (2020).

[30] A. Zoufaly, M. Poglitsch, J.H. Aberle, W. Hoepler, T. Seitz, M. Traugott, A. Grieb, E. Pawelka, H. Laferl, C. Wenisch, S. Neuhold, D. Haider, K. Stiasny, A. Bergthaler, E. Puchhammer-Stoeckl, A. Mirazimi, N. Montserrat, H. Zhang, A.S. Slutsky, J. M. Penninger, Human recombinant soluble ACE2 in severe COVID-19, Lancet Respir. Med. 8 (11) (2020) 1154–1158.

[31] A. Acharya, K. Pandey, M. Thurman, E. Klug, J. Trivedi, K. Sharma, C.L. Lorson, K. Singh, S.N. Byrareddy, Discovery and evaluation of entry inhibitors for SARS-CoV-2 and its emerging variants, J. Virol. 95 (24) (2021), e0143721.

[32] Y.H. Shin, K. Jeong, J. Lee, H.J. Lee, J. Yim, J. Kim, S. Kim, S.B. Park, Inhibition of ACE2-spike interaction by an ACE2 binder suppresses SARS-CoV-2 entry, Angew. Chem. 61 (11) (2022), e202115695.

[33] C.B. Jackson, M. Farzan, B. Chen, H. Choe, Mechanisms of SARS-CoV-2 entry into cells, Nat. Rev. Mol. Cell Biol. 23 (1) (2022) 3–20.

[34] H. Yeh, D.N.K. Vo, Z.H. Lin, H.P.T. Ho, W.J. Hua, W.L. Qiu, M.H. Tsai, T.Y. Lin, GMI, a protein from Ganoderma microsporum, induces ACE2 degradation to alleviate infection of SARS-CoV-2 Spike-pseudotyped virus, Phytomedicine: Int. J. Phytother. Phytopharm. 103 (2022), 154215.

[35] F.a.D. Administration, NDI 1133 - Ganoderma Micro Immunomodulatory Protein (GMI) Tomilab LLC (2020). ⟨https://www.regulations.gov/document/FDA-2020-S-0023-0006⟩.

[36] J.M. Chou, J.L. Tsai, J.N. Hung, I.H. Chen, S.T. Chen, M.H. Tsai, The ORF8 protein of SARS-CoV-2 modulates the spike protein and its implications in viral transmission, Front. Microbiol. 13 (2022), 883597.

[37] W.F. Garcia-Beltran, K.J. Denis St, A. Hoelzemer, E.C. Lam, A.D. Nitido, M. L. Sheehan, C. Berrios, O. Ofoman, C.C. Chang, B.M. Hauser, J. Feldman, A. L. Roederer, D.J. Gregory, M.C. Poznansky, A.G. Schmidt, A.J. Iafrate, V. Naranbhai, A.B. Balazs, mRNA-based COVID-19 vaccine boosters induce neutralizing immunity against SARS-CoV-2 Omicron variant, Cell 185 (3) (2022) 457–466, e4.

[38] S.B. Park, P. Irvin, Z. Hu, M. Khan, X. Hu, Q. Zeng, C. Chen, M. Xu, M. Leek, R. Zang, J.B. Case, W. Zheng, S. Ding, T.J. Liang, Targeting the fusion process of SARS-CoV-2 infection by small molecule inhibitors, mBio (2022), e0323821.

[39] H.Y. Fu, R.S. Hseu, Safety assessment of the fungal immunomodulatory protein from Ganoderma microsporum (GMI) derived from engineered Pichia pastoris:

Genetic toxicology, a 13-week oral gavage toxicity study, and an embryo-fetal developmental toxicity study in Sprague-Dawley rats, Toxicology Reports 9 (2022) 1240–1254.
[40] M. Hoffmann, N. Krüger, S. Schulz, A. Cossmann, C. Rocha, A. Kempf, I. Nehlmeier, L. Graichen, A.S. Moldenhauer, M.S. Winkler, M. Lier, A. Dopfer-Jablonka, H. M. Jäck, G.M.N. Behrens, S. Pöhlmann, The Omicron variant is highly resistant against antibody-mediated neutralization: Implications for control of the COVID-19 pandemic, Cell 185 (3) (2022) 447–456, e11.
[41] Y. Liu, J. Liu, K.S. Plante, J.A. Plante, X. Xie, X. Zhang, Z. Ku, Z. An, D. Scharton, C. Schindewolf, S.G. Widen, V.D. Menachery, P.Y. Shi, S.C. Weaver, The N501Y spike substitution enhances SARS-CoV-2 infection and transmission, Nature 602 (7896) (2022) 294–299.
[42] Y. Zhang, T. Zhang, Y. Fang, J. Liu, Q. Ye, L. Ding, SARS-CoV-2 spike L452R mutation increases Omicron variant fusogenicity and infectivity as well as host glycolysis, Signal Transduct. Target. Ther. 7 (1) (2022) 76.
[43] B. Korber, W.M. Fischer, S. Gnanakaran, H. Yoon, J. Theiler, W. Abfalterer, N. Hengartner, E.E. Giorgi, T. Bhattacharya, B. Foley, K.M. Hastie, M.D. Parker, D. G. Partridge, C.M. Evans, T.M. Freeman, T.I. de Silva, C. McDanal, L.G. Perez, H. Tang, A. Moon-Walker, S.P. Whelan, C.C. LaBranche, E.O. Saphire, D. C. Montefiori, Tracking changes in SARS-CoV-2 spike: evidence that D614G increases infectivity of the COVID-19 virus, Cell 182 (4) (2020) 812–827, e19.
[44] J.A. Plante, Y. Liu, J. Liu, H. Xia, B.A. Johnson, K.G. Lokugamage, X. Zhang, A. E. Muruato, J. Zou, C.R. Fontes-Garfias, D. Mirchandani, D. Scharton, J.P. Bilello, Z. Ku, Z. An, B. Kalveram, A.N. Freiberg, V.D. Menachery, X. Xie, K.S. Plante, S. C. Weaver, P.Y. Shi, Spike mutation D614G alters SARS-CoV-2 fitness, Nature 592 (7852) (2021) 116–121.
[45] C. Zeng, J.P. Evans, T. King, Y.M. Zheng, E.M. Oltz, S.P.J. Whelan, L.J. Saif, M. E. Peeples, S.L. Liu, SARS-CoV-2 spreads through cell-to-cell transmission, Proc. Natl. Acad. Sci. USA 119 (1) (2022).
[46] Q. Sattentau, Avoiding the void: cell-to-cell spread of human viruses, Nat. Rev. Microbiol. 6 (11) (2008) 815–826.
[47] W. Mothes, N.M. Sherer, J. Jin, P. Zhong, Virus cell-to-cell transmission, J. Virol. 84 (17) (2010) 8360–8368.
[48] K.M. Law, N. Satija, A.M. Esposito, B.K. Chen, Cell-to-cell spread of HIV and viral pathogenesis, Adv. Virus Res. 95 (2016) 43–85.
[49] B.M. Dale, G.P. McNerney, D.L. Thompson, W. Hubner, K. de Los Reyes, F. Y. Chuang, T. Huser, B.K. Chen, Cell-to-cell transfer of HIV-1 via virological synapses leads to endosomal virion maturation that activates viral membrane fusion, Cell host Microbe 10 (6) (2011) 551–562.
[50] G. Beucher, M.L. Blondot, A. Celle, N. Pied, P. Recordon-Pinson, P. Esteves, M. Faure, M. Métifiot, S. Lacomme, D. Dacheux, D.R. Robinson, G. Längst, F. Beaufils, M.E. Lafon, P. Berger, M. Landry, D. Malvy, T. Trian, M.L. Andreola, H. Wodrich, Bronchial epithelia from adults and children: SARS-CoV-2 spread via syncytia formation and type III interferon infectivity restriction, Proc. Natl. Acad. Sci. USA 119 (28) (2022), e2202370119.
[51] L. Lin, Q. Li, Y. Wang, Y. Shi, Syncytia formation during SARS-CoV-2 lung infection: a disastrous unity to eliminate lymphocytes, Cell death Differ. 28 (6) (2021) 2019–2021.
[52] B. Rockx, T. Kuiken, S. Herfst, T. Bestebroer, M.M. Lamers, B.B. Oude Munnink, D. de Meulder, G. van Amerongen, J. van den Brand, N.M.A. Okba, D. Schipper, P. van Run, L. Leijten, R. Sikkema, E. Verschoor, B. Verstrepen, W. Bogers, J. Langermans, C. Drosten, M. Fentener van Vlissingen, R. Fouchier, R. de Swart, M. Koopmans, B.L. Haagmans, Comparative pathogenesis of COVID-19, MERS, and SARS in a nonhuman primate model, Sci. (N. Y., N. Y.) 368 (6494) (2020) 1012–1015.
[53] J. Buchrieser, J. Dufloo, M. Hubert, B. Monel, D. Planas, M.M. Rajah, C. Planchais, F. Porrot, F. Guivel-Benhassine, S. Van der Werf, N. Casartelli, H. Mouquet, T. Bruel, O. Schwartz, Syncytia formation by SARS-CoV-2-infected cells, EMBO J. 40 (3) (2021), e107405.
[54] Q. Li, J. Nie, J. Wu, L. Zhang, R. Ding, H. Wang, Y. Zhang, T. Li, S. Liu, M. Zhang, C. Zhao, H. Liu, L. Nie, H. Qin, M. Wang, Q. Lu, X. Li, J. Liu, H. Liang, Y. Shi, Y. Shen, L. Xie, L. Zhang, X. Qu, W. Xu, W. Huang, Y. Wang, SARS-CoV-2 501Y.V2 variants lack higher infectivity but do have immune escape, Cell 184 (9) (2021), 2362-2371.e9.
[55] Y. Liu, L.M. Yan, L. Wan, T.X. Xiang, A. Le, J.M. Liu, M. Peiris, L.L.M. Poon, W. Zhang, Viral dynamics in mild and severe cases of COVID-19, Lancet Infect. Dis. 20 (6) (2020) 656–657.
[56] J. Fajnzylber, J. Regan, K. Coxen, H. Corry, C. Wong, A. Rosenthal, D. Worrall, F. Giguel, A. Piechocka-Trocha, C. Atyeo, S. Fischinger, A. Chan, K.T. Flaherty, K. Hall, M. Dougan, E.T. Ryan, E. Gillespie, R. Chishti, Y. Li, N. Jilg, D. Hanidziar, R.M. Baron, L. Baden, A.M. Tsibris, K.A. Armstrong, D.R. Kuritzkes, G. Alter, B. D. Walker, X. Yu, J.Z. Li, SARS-CoV-2 viral load is associated with increased disease severity and mortality, Nat. Commun. 11 (1) (2020) 5493.
[57] C. Chakraborty, A.R. Sharma, M. Bhattacharya, G. Agoramoorthy, S.S. Lee, The drug repurposing for COVID-19 clinical trials provide very effective therapeutic combinations: lessons learned from major clinical studies, Front. Pharmacol. 12 (2021), 704205.
[58] X. Wang, Y. Guan, COVID-19 drug repurposing: a review of computational screening methods, clinical trials, and protein interaction assays, Med. Res. Rev. 41 (1) (2021) 5–28.
[59] S. Kumar, S. Kovalenko, S. Bhardwaj, A. Sethi, N.Y. Gorobets, S.M. Desenko, B. Poonam, Rathi, Drug repurposing against SARS-CoV-2 using computational approaches, Drug Discov. Today 27 (7) (2022) 2015–2027.
[60] W.D. Jang, S. Jeon, S. Kim, S.Y. Lee, Drugs repurposed for COVID-19 by virtual screening of 6,218 drugs and cell-based assay, Proc. Natl. Acad. Sci. USA 118 (30) (2021).
[61] M.A. Bakowski, N. Beutler, K.C. Wolff, M.G. Kirkpatrick, E. Chen, T.H. Nguyen, L. Riva, N. Shaabani, M. Parren, J. Ricketts, A.K. Gupta, K. Pan, P. Kuo, M. Fuller, E. Garcia, J.R. Teijaro, L. Yang, D. Sahoo, V. Chi, E. Huang, N. Vargas, A.J. Roberts, S. Das, P. Ghosh, A.K. Woods, S.B. Joseph, M.V. Hull, P.G. Schultz, D.R. Burton, A. K. Chatterjee, C.W. McNamara, T.F. Rogers, Drug repurposing screens identify chemical entities for the development of COVID-19 interventions, Nat. Commun. 12 (1) (2021) 3309.
[62] W.K.B. Chan, K.M. Olson, J.W. Wotring, J.Z. Sexton, H.A. Carlson, J.R. Traynor, In silico analysis of SARS-CoV-2 proteins as targets for clinically available drugs, Sci. Rep. 12 (1) (2022) 5320.
[63] D. Goletti, F. Cantini, Baricitinib Therapy in Covid-19 Pneumonia - An unmet need fulfilled, N. Engl. J. Med. 384 (9) (2021) 867–869.
[64] K.T. Peng, J.L. Chen, L.T. Kuo, P.A. Yu, W.H. Hsu, C.W. Lee, P.J. Chang, T. Y. Huang, GMI, an Immunomodulatory Peptide from Ganoderma microsporum, Restrains Periprosthetic Joint Infections via Modulating the Functions of Myeloid-Derived Suppressor Cells and Effector T Cells, Int. J. Mol. Sci. 22 (13) (2021).
[65] M. Haak-Frendscho, K. Kino, T. Sone, P. Jardieu, Ling Zhi-8: a novel T cell mitogen induces cytokine production and upregulation of ICAM-1 expression, Cell. Immunol. 150 (1) (1993) 101–113.
[66] H.Y. Hsu, K.F. Hua, W.C. Wu, J. Hsu, S.T. Weng, T.L. Lin, C.Y. Liu, R.S. Hseu, C. T. Huang, Reishi immuno-modulation protein induces interleukin-2 expression via protein kinase-dependent signaling pathways within human T cells, J. Cell. Physiol. 215 (1) (2008) 15–26.